Crack propagation in high-temperature granite after cooling shock: experiment and numerical simulation

Yan-jun Shen[1,2] · Jian-shuai Hao[2] · Xin Hou[3] · Jiang-qiang Yuan[4] · Zhi-peng Bai[2]

Abstract

Achieving crack propagation and rapid deterioration of high-temperature rock masses by using cooling shocks is important for improving the efficiency of low-permeability oil and gas production, geothermal well pumping, and other engineering facilities. In this study, the temperatures of four groups of granite samples with holes were set as 150, 350, 550, and 750 °C. To study the crack propagation in high-temperature granite suffering from different cooling shocks, the cooling shock temperatures were set as −20, 0, 20, and 25 °C in experiments and an RFPA^{2D}-Thermal numerical simulation. The results indicated that in the range of 350–550 °C, there is a critical temperature for the sudden change of the crack macroscopic shape. Numerous open cracks appeared on the rock surface, and the thermal damage caused by the cooling shocks was significantly enhanced within the temperature range. Additionally, under the action of the cooling shocks, cracks were initiated in the high-temperature granite at the boundary of the cooling shock hole and the sample and extended radially to the interior of the sample. Moreover, in the process of crack propagation, there was always an annular heat-balance zone inside the rock. Thus, the cracks generated at the boundary of the cube are not connected to the cracks formed at the center hole. A larger temperature gradient in the rock led to a higher crack propagation rate, larger penetration depth, and higher density of cooling-induced cracks. The results of this study can not only improve the permeability of reservoir rocks but also have important reference value for rock engineering in high-temperature environments.

Introduction

With the depletion of traditional fossil energy, abundant eco-friendly geothermal energy resources are becoming an important energy supplement. However, in the process of mining thermal reservoir granite, the artificial thermal reservoir structure still faces the problems of penetrating the replacement path and increasing the heat-exchange area to improve the utilization rate. The hydraulic fracturing method can only increase the crack length of the original thermal reservoir granite and improve the heat-exchange efficiency to limited degrees. Therefore, to solve the problem of large-scale through cracks in thermal reservoirs, increase the crack density, and improve the extraction efficiency of hot dry rock, it is important to study the crack propagation in high-temperature granite under cooling shocks.

Researchers have conducted many laboratory experiments and numerical simulations on the fracture process of high-temperature rocks. These studies indicated that the initiation, propagation, and coalescence of internal cracks in rocks are

Highlight
1. The crack propagation and deterioration mechanism of different high-temperature granite after cooling shocks are revealed by multiple ways.
2. The differences of cooling shock crack propagation between laboratory experiment and numerical simulation are discussed and analyzed.
3. The entire process of a granite cooling shock crack from initiation to propagation and coalescence is studied by numerical simulation, and the crack density on the rock surface under real time condition is calculated.

✉ Yan-jun Shen
   shenyj@xust.edu.cn

1 Geological Research Institute for Coal Green Mining, Xi'an University of Science and Technology, Xi'an 710054, China

2 College of Geology and Environment, Xi'an University of Science and Technology, Xi'an 710054, China

3 ShanDong Electric Power Engineering Consulting Institute Corp., LTD, Jinan 250013, China

4 Nuclear Industry Jingxiang Construction Group Co.,Ltd., Huzhou 313002, China

the main reasons for the deformation of intact rocks (Cai et al. 2004; Cui et al. 2019; Zhang et al. 2015). It is helpful to study the failure mechanism of rocks by analyzing the initiation, propagation, and coalescence of cracks at the microscale (Diederichs et al. 2004; Liu et al. 2015; Zhang et al. 2017). In this regard, researchers have used acoustic emission (AE) to conduct a large number of studies on rock strength and related microcracks (Kumari et al. 2018a; Siratovich et al. 2015; Zhu et al. 2018), scanning electron microscopy (SEM) (Ghamartale et al. 2019; Liu et al. 2018; Lyu et al. 2018), and computed tomography (CT) (Li et al. 2019; Zhao and Zhou 2020); the results indicate that the shapes, size distribution, and composition of minerals significantly affect the strength and microcrack process of rocks. Zhou et al. (2020) examined a thin layer via SEM and analyzed the thermal damage mechanism of granite and the thermally induced microcracks in granite, funding that intergranular cracks and intragranular cracks propagated most intensively at 400–700 °C. Akdag et al. (2018, 2020) explored the effect of thermal damage (25–150 °C) on the strain rupture characteristics of brittle rocks and the energy characteristics of quasi-static fracture of granite under true triaxial loading and unloading conditions using acoustic emission and kinetic energy analysis and proposed a strain impact susceptibility criterion for brittle rocks based on energy release rate. Miao et al. (2020) explored that thermally induced microcracking was the underlying cause of changes in physical and mechanical behavior and fracture characteristics of granites above 500 °C and that microcrack density, connectivity, and crack opening increased with increasing temperature. Feng et al. (2020) studied the fracture characteristics of fine-grained granites in geothermal reservoirs and found that the interconnection of intracrystalline and intercrystalline cracks leads to the fracture of granite structures. Piane et al. (2015) quantified the unit surface density or volume, aspect ratio, and average length of microcracks and found heat treatment opened the grain boundaries and did not generate intragranular cracks. Additionally, numerical simulations of rock fracture have yielded rich results. Bažant et al. (1979) used numerical simulation method to study the thermal shock of dry granite. Huang et al. (2020) investigated the mechanical properties and mechanism of granite at a high temperature and high cooling rates via numerical simulations and examined the effects of preexisting defects on the mechanical behavior of granite. Cha et al. (2014) performed a simulation experiment on the low-temperature fracture of a model material induced by liquid nitrogen. Gao et al. (2016) performed numerical simulations on the microstructure of brittle rock based on a discrete-element model for a fragile particle. Zhang et al. (2018b) examined the characteristics of the grain size and described the deformation, fracture, and fracture process of model elements in detail.

To solve the problem of the low pumping efficiency in geothermal exploitation, low-temperature fracturing is often used for energy exchange in practical engineering, which inevitably involves heat exchange between low-temperature liquid and high-temperature rock. The cooling conditions significantly affect the physical and mechanical properties of the rock after heat treatment, and the deterioration of rocks caused by rapid cooling (water cooling or liquid nitrogen cooling) is more serious than that caused by slow cooling (such as air cooling) or furnace cooling (Wu et al. 2019; Zhao et al. 2018). Isaka et al. (2018) performed rapid water cooling treatments on granite at different temperatures and found that the thermal degradation effect under rapid cooling was far stronger than that under slow cooling. Shi et al. (2020) and Weng et al. (2020) studied the effects of cyclic heating and water cooling strips on the mechanical properties and cracking characteristics of granite. The results indicated that thermal stress was the main factor causing the deterioration of the granite after heat treatment, with the number of thermal cycles increased. The width, length, and number of transgranular microcracks gradually increased, and the strength and stiffness of the rock decreased significantly. Zhang et al. (2018a, b) and Huang et al. (2019) studied the effects of liquid nitrogen on the rock-breaking effect and rock deterioration. Shen et al. (2020a, b, 2019) performed cooling shock experiments on granite samples and examined the influence of cooling shock on the physical and mechanical properties of high-temperature granite through various experimental methods. Tang et al. (2001) and Tang et al. (2020) investigated the low-temperature fracture phenomenon of rock under thermal shock theoretically and via numerical simulations. They studied the crack propagation process of the rock under cooling impact and analyzed the effects of relevant parameters on the rock temperature and minimum principal stress distribution.

The current research focuses on the mechanical damage, cooling methods, and cooling shocks effect of high-temperature rock. However, few studies have been performed on the cooling crack propagation and related numerical simulations after low-temperature rapid cooling. Thus, in the present study, the crack propagation in high-temperature granite under cooling shocks was analyzed via laboratory experiments and numerical simulations, and the thermal damage mechanism in the process of cooling shock crack growth was examined at the microscale.

Experiment and analysis

Experimental preparation and procedure

The samples used in this experiment were taken from the same rock stratum in Ganzi, Sichuan Province. The granite sample
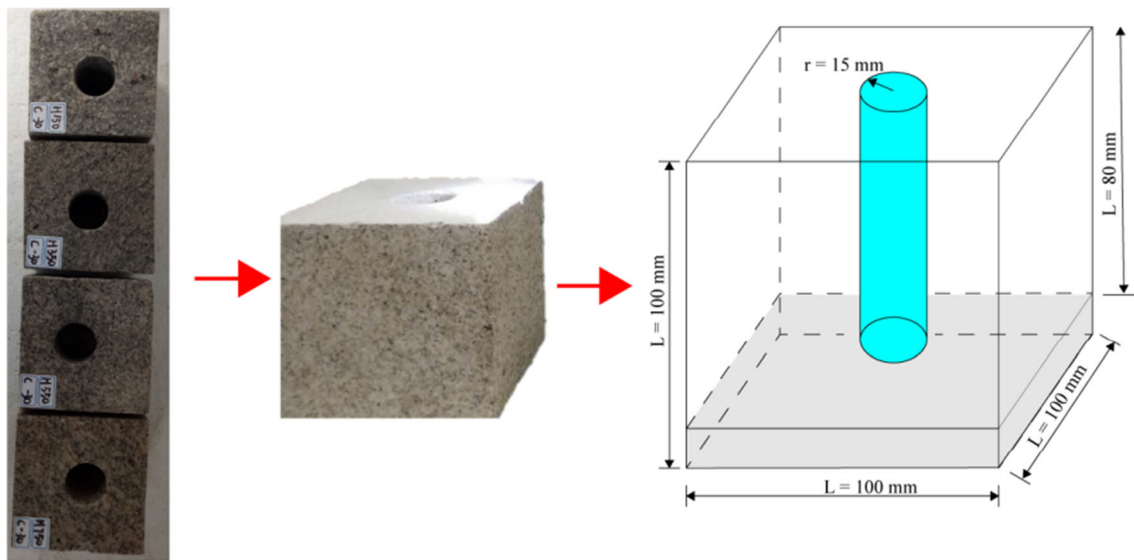
Fig. 1 Morphology and size of granite with holes

size is a cube of 100 mm, the drilling depth was 80 mm, and the diameter was 30 mm (as shown in Fig. 1). Calcium chloride solution was selected as refrigerant; DW-40 low-temperature experiment chamber was used to lower the solution to 20 °C, 0 °C, and −20 °C, respectively; BLMT-1200 °C high-temperature and energy-saving box furnace was used for initial heating of granite; the detailed experimental procedure are as follows: first, the granite was heated to 150, 350, 550, and 750 °C by BLMT-1200 °C high-temperature box furnace, and the rate was 5 °C/min to avoid the rock caused by too fast heating varying degrees of damage. In order to make the inside of the granite heat evenly, when the temperature of the granite reaches the preset temperature, the temperature was kept constant for 4 h. For the treatment of the cold extract solution, the calcium chloride solution was cooled down to 20 °C, 0 °C, and −20 °C, respectively, by a DW-40 low-temperature test chamber and then thermostated for 8 h after reaching the target temperature. After that, the heated granite was quickly taken out, and calcium chloride solution with different temperatures was injected into the reserved holes of granite for cooling shock test. At the same time, a group of heated granite was naturally cooled. The experiment process is shown in Fig. 2.

Experimental results and analysis

Under the action of cooling shocks, the high-temperature granite was damaged to different extents. The temperature difference between the high-temperature rock and the cold medium at 150 °C is so small that there is almost no cracking on the rock surface, so the cooling shock effect on the granite

at 150 °C is almost absent. At 350 °C, a large number of microcracks appear on the surface of granite, which are mainly caused by the effect of high temperature, and the different temperatures (0 °C, 20 °C, −20 °C) caused by the cold medium on the granite caused by the cooling shock effect become a secondary factor; the influence effect is relatively small, so the effect of cooling shock on granite at 350 °C is also insignificant. The granite at 550 and 750 °C exhibited significant differences under the cooling shocks. We used Particles (Pores) and Cracks Analysis System (PCAS) software for image extraction and analysis, and the PCAS software is a professional software for the identification and quantitative analysis of pore systems and cracks systems (Liu et al. 2011, 2013). The software can automatically identify various pores and fractures in the image and obtain various geometric parameters and statistical parameters, as well as import various fracture images, and automatically binarize the images, and then output fissure geometric and statistical parameters, display vector images and rose diagrams, etc. (Liu et al. 2020; Qin et al. 2018). The fracture conditions of granite at different temperatures are presented in Table 1.

Table 1 shows the cracking of granite at different temperatures. The 150 °C granite group exhibited a poor rock fracture effect and did not exhibited a difference under the action of cooling shocks. Microcracks began to appear on the granite surface at 350 °C. The lengths and widths of the cracks were very small, and the cooling shock effect was not obvious. With an increase in the initial temperature of the granite, the cracking effect caused by the cooling shocks changed. The surface cracks and width of the granite at 550 and 750 °C increased gradually, there was a visible dense network of microcracks, and locally open cracks were formed at the rock
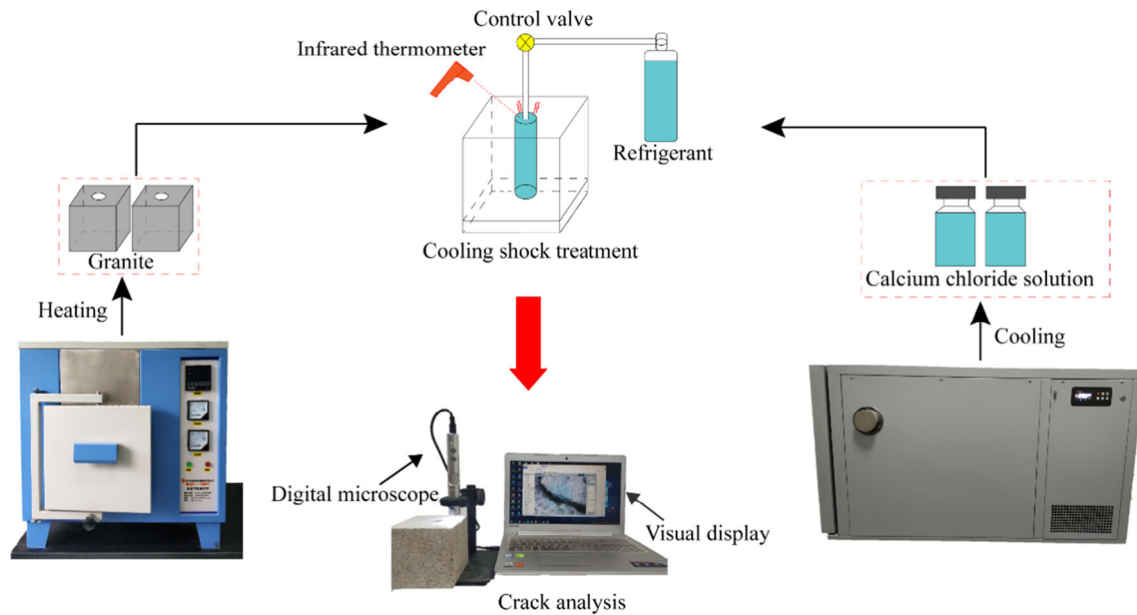
Fig. 2 Cooling shock experimental process of high-temperature granite

surface. Cracks in granite at 550 °C usually propagate around mineral particles, resulting in more circumferential cracks. Due to the large thermal shock on the granite surface at 750°C, the circumferential cracks propagate along the grain boundary and form radial cracks. Additionally, as the rock temperature rises and the refrigerant temperature decreases, the cracks at the round holes and outer boundaries of the rock develop and penetrate each other, forming penetrating cracks from the holes all the way through to the outer boundaries of the rock sample. Figure 3 shows the area ratio of cracks and voids to the total surface (subtracted by the area of the central hole) identified by the software (PCAS). With the rise of rock temperature, the proportion of cracks on rock surface increases significantly, and the cracking effect is more obvious with the decrease of refrigerant temperature. Regarding the macroscopic crack opening area, morphology, and deterioration effect of the rock, the cracking effect of the −20 °C cooling shock group was better than that of the 0 °C cooling shock group, and the cracking effect of the 0 °C group was better than that of the 20 °C group.

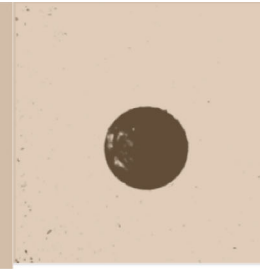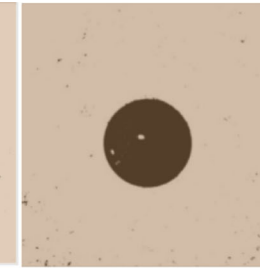## Numerical simulation and analysis of crack propagation
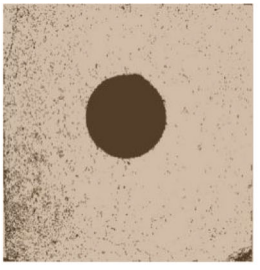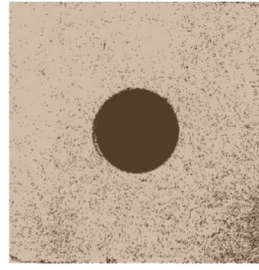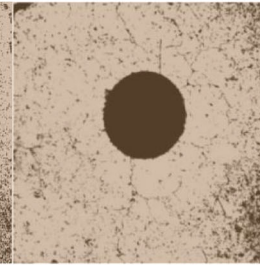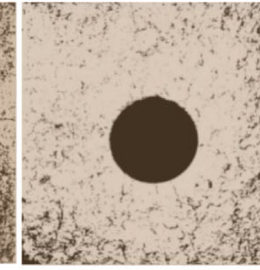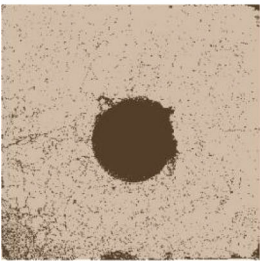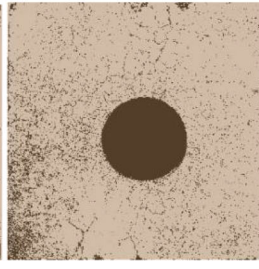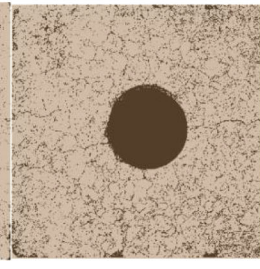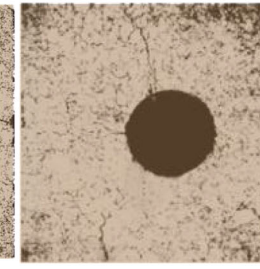
Model and parameters

Realistic failure process analysis (RFPA) is a numerical simulation method based on finite element theory and statistical damage theory, which can well simulate the progressive fracture growth in rocks by fully considering the characteristics of nonlinearity, nonuniformity, and

anisotropy accompanying the rock rupture process (Tang et al. 2015; Dalian Mechsoft Co L 2016). For example, Tang et al. (2006, 2016) and Huang et al. (2001) simulated the thermal fracture behavior of other brittle solids such as rocks under the action of thermal shock using the RFPA^{2D} program, and the simulation results were in good agreement with the experimental results. In this paper, in order to further investigate the crack expansion law of high-temperature granite under the action of cooling shock, the RFPA^{2D}-Thermal model, a temperature module of RFPA, was used to analyze the thermal rupture process and mechanism of the material from the perspective of fine mechanics (Zhu et al. 2003), and the rock crack extension process was simulated numerically.
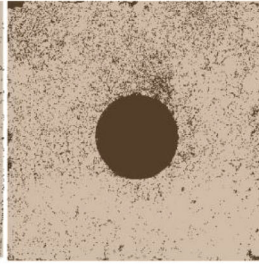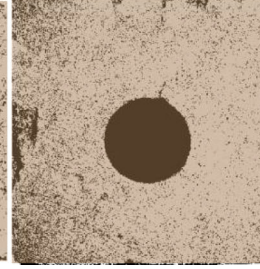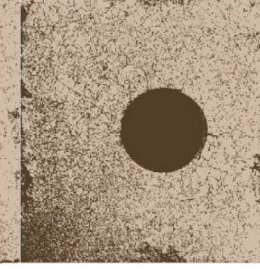
According to the RFPA primitive assignment principle, we need to consider the rock's tensile and compressive strength, elastic modulus, Poisson's ratio, and the angle of internal friction. Based on the RFPA^{2D}-Thermal model, we also need to consider the rock's thermal conductivity, volumetric heat capacity, coefficient of thermal expansion, convection heat transfer coefficient, and other thermodynamic parameters of the rock. Rock's compressive strength, modulus of elasticity, and Poisson's ratio of granite after high temperature were obtained by uniaxial test (WAW-1000 universal testing machine), and the internal friction angle and tensile strength of granite were obtained by triaxial compression test (HTC605A microcomputer-controlled electro-hydraulic servo pressure tester) and Brazilian splitting test (MTS815 triaxial testing machine), respectively. The thermal conductivity and volumetric heat capacity were determined using a hot-disk instrument, and the coefficient of thermal expansion and convection heat-transfer coefficient were obtained from the results of Wang,

Table 1 Results of granite surface crack experiments with different cooling shocks

Temperature	Natural cooling	Cooling shock 20 °C	Cooling shock 0 °C	Cooling shock −20 °C
150 °C				
350 °C				
550 °C				
750 °C				

Xu, Zhu, etc. (Wang and Konietzky 2019; Xu et al. 2014; Zhu et al. 2019); the physical and mechanical properties of the sample elements are presented in Table 2.

The size of the rock model was 100 mm × 100 mm, and there was a hole with a diameter of 30 mm in the middle. The model was divided into 90000 elements. The total number of steps was 100, and the initial temperature of the model was set as 150, 350, 550, and 750 °C. The sample boundary temperature (the first type of boundary condition) was uniform (25 °C), and the inner boundary temperature (the third type of boundary condition) was set as 20, 0, and −20 °C. A

simulation experiment of the cooling shock was conducted. The case of a 0 °C cooling shock acting on 150 °C granite was considered as an example. First, the 100 mm × 100 mm granite model was divided into 300 × 300 units, and the relevant physical and mechanical parameters of the rock elements were set. The initial temperature of the model was 150 °C. A hole with a diameter of 30 mm was formed, and the hole temperature inside the hole was set to 0 °C. Finally, the external boundary of the model was set as 25 °C. After the establishment of the model, the simulation experiment of the fracture was performed. The tensile and compressive strengths, elastic
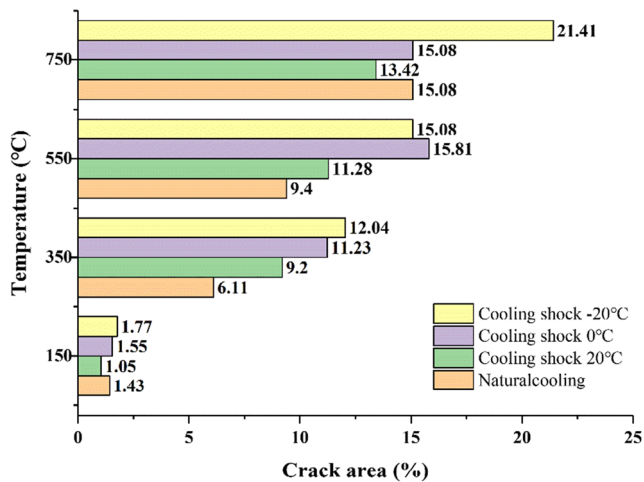
Fig. 3 Surface crack area ratios of granite under different cooling shocks

modulus, angle of internal friction, and Poisson's ratio were determined through laboratory experiments and relevant calculations.

Simulation of crack growth behavior of granite

The RFPA^{2D}-Thermal was used to simulate the entire process of a granite cooling shock crack from initiation to propagation and coalescence. The common features of crack propagation were as follows: the crack initiation in the high-temperature granite started at the boundary of the cooling shock hole and extended radially to the interior of the rock. The distance between the medium length crack and long cracks was almost equal. Cracks also appeared at the sample boundary of the rock contact, and the cracks propagated perpendicularly to the rock boundary toward the rock interior. With increasing calculation steps, the internal and external cracks of the model propagated synchronously, and the cracks continued to develop and expand. Meanwhile, a dynamic equilibrium zone was formed, and the rock particles in the equilibrium zone were in thermal equilibrium and were not influenced by the cooling

shock temperature field with the breaking of the dynamic equilibrium region. Internal and external cracks were connected, forming a network. The number of cracks and their size increased, and the rock gradually deteriorated. Owing to the length limitations of this article, the models with 150, 350, 550, and 750 °C granite under a –20 °C cooling shock were considered as examples to analyze the crack propagation in detail. The cracking situations of the granite are presented in Table 3.

Steps 0–10 (initiation stage): Fine cracks were generated at both the cooling shock boundary (inner boundary) and the room boundary (sample boundary) of the rock model. The inner boundary cracks propagated toward the interior of the rock perpendicularly to the cooling shock boundary, and the sample boundary crack propagated perpendicularly toward the interior of the rock. The cracks were short and fine at this stage.

Steps 10–30 (early stage of propagation): The inner and sample boundary cracks propagated from the temperature boundary radially toward the interior of rock. Microcracks expanded and combined with each other, forming longer and wider cracks. The differences were as follows: the length, width, and spacing of the generated cracks in the 150 °C rock model were uniform, whereas the lengths and widths of the cracks in the other three rock temperature groups differed significantly, and the round cooling shock hole began to deform.

Steps 30–70 (later stage of propagation): The internal and external cracks of the 150 °C rock model were fully expanded, and the main and secondary cracks were continuously connected and fused into a network distribution. Additionally, a local ring-shaped equilibrium area was formed. The rock elements in the equilibrium area were in a thermal equilibrium state, and the rock particles were not damaged. Owing to the nonuniform expansion of the model particles, the rocks at 350, 550, and 750 °C exhibited obvious shrinkage deformation at the local part of the circular hole, with the heat-balance zone further shrinking. The internal and external cracks began to

Table 2 Physical and mechanical properties of the sample elements

Granite temperature (°C)	150	350	550	750
Elastic modulus (GPa)	32	22	18	13
Compressive strength (MPa)	94.6	78.8	45.5	33.8
Tensile strength (MPa)	9.5	7.5	4.5	2.8
Poisson's ratio	0.18	0.14	0.07	0.04
The angle of internal friction (°)	30.3	30.5	28.5	25
Thermal conductivity (W/(m·K))	1.08	1.01	0.8	0.7
Volumetric heat capacity (J/(m^3·K)10^6)	1.63	1.6	1.59	1.57
Coefficient of thermal expansion (10^{-6} °C^{-1}) (Wang and Konietzky 2019; Xu et al. 2014)	7.88	10.47	16.66	3.40
Convection heat transfer coefficient ((W/ (m^2·K)) (Zhu et al. 2019)	235.87	232.28	220.83	214.99

Table 3 Stress diagram of the surface crack propagation process of granite under cooling shocks

Step	150 °C granite	350 °C granite	550 °C granite	750 °C granite
0				
10				
30				
70				
100				
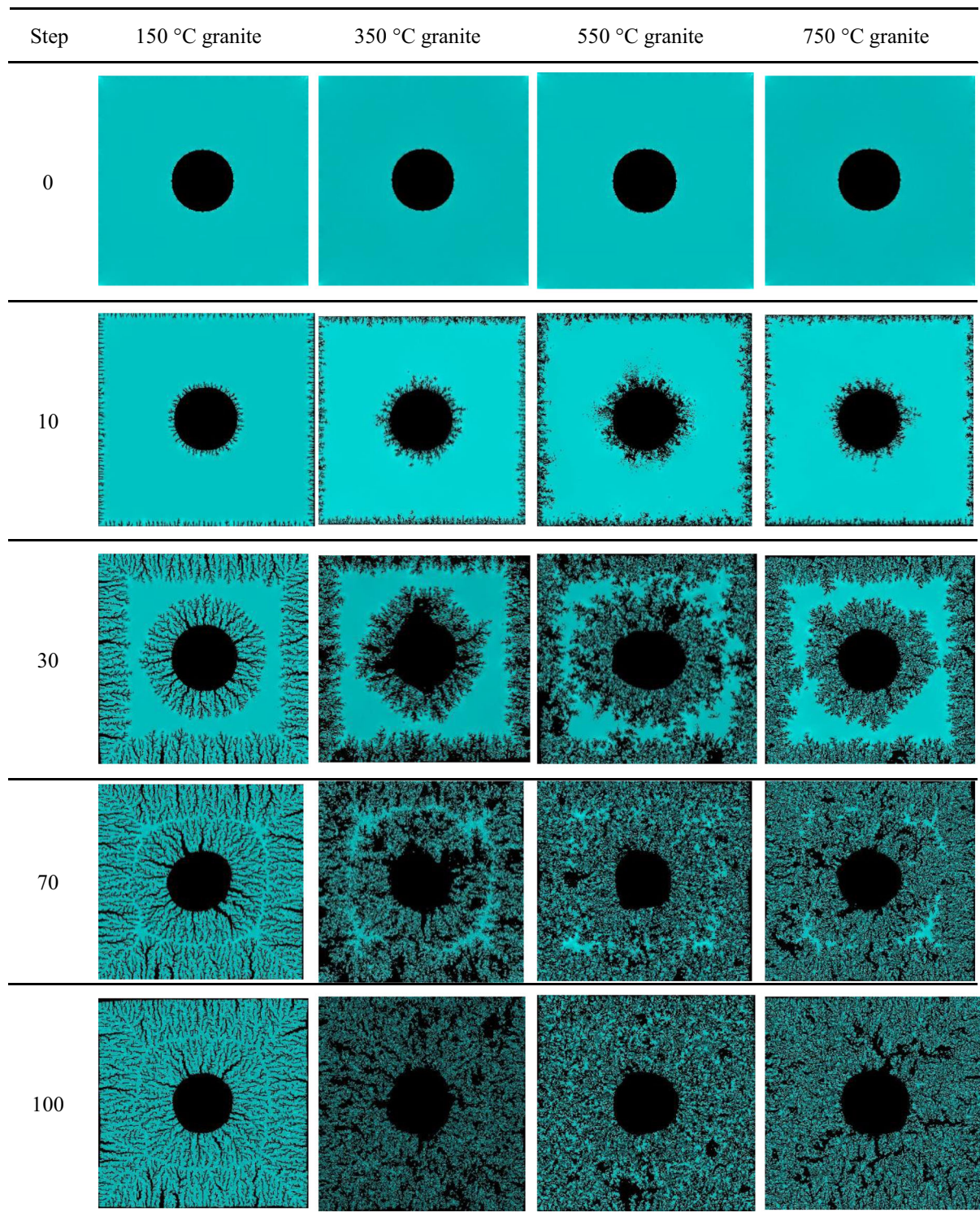
propagate and fuse locally. There were many cavity structures in the interior and boundary of the rock model. The whole rock model deteriorated significantly.

Steps 70–100 (coalescence stage): The cooling shock cracks of the rock model with various temperature gradients have basically completed and transitioned to each other. The damage effect was relatively obvious for the rocks at 150 and

350 °C. Lin (2002) found that the critical temperature of thermal microcracks in Inada granite was 100–125 °C. In this temperature range, the α-β transition of quartz and the continuous generation of thermal microcracks occur. When the granite temperature is 350 °C, the microcracks further propagated into cracks, and new microcracks sprout around the cracks. The network microcracks formed were more obvious in 350 °C granite than in 150 °C granite, and some small cavities also appeared locally. The damage to the rock model at 550 °C was severe, in agreement with the results of Shi et al. (2020). The fracture development of the rock at 550 °C was well propagated relatively, forming a clastic structure, and the cavity structure was increased in size. For the 750 °C granite, the effect of tension fracture was more obvious. The fracture was connected thoroughly. Some closed fractures were formed, and the rock was broken into small pieces and a clastic shape in a large area. There were more voids and cavity structures in 750 °C rock than in 550 °C rock.

To further investigate the crack propagation in high-temperature granite under cooling shocks, the real-time proportion of the cooling shock cracks on the rock surface was calculated as the number of steps increased (as shown in Fig. 4). Steps 0–10: The cracks initiated rapidly, resulting in a large

number of microcracks. Steps 10–70: The rock cracks were in the early stage of propagation. The temperature field of the cooling shock moved to the inside of the rock owing to the increase in microcracks, and the crack propagation speed initially increased. With further movement of the temperature field to the inside of the rock, the temperature gradient in the rock decreased, and the rock particles gradually reached a thermal equilibrium state, reducing the crack growth rate. Finally, the crack propagation process was complete. Step 70–100: With the breaking of the internal thermal equilibrium state of the rock, the internal and external cracks penetrated and fuse with each other, and the proportion of the crack surface increased.

Regarding the effect of crack propagation, the proportion of surface cracks of the rock at 750 °C was as large as 29% under the action of a cooling shock of –20 °C, but only 5.43% of the rock surface cracked for the 150 °C granite, and the proportion of surface cracks for the 750 °C granite under the natural cooling temperature was only 17%. The crack growth rate was examined in each stage, for the cooling shock temperature of –20 °C. The crack growth rate in each stage was the highest at the granite temperature of 750 °C, followed by 550 and 350 °C, and was the lowest at 150 °C. Thus, a larger
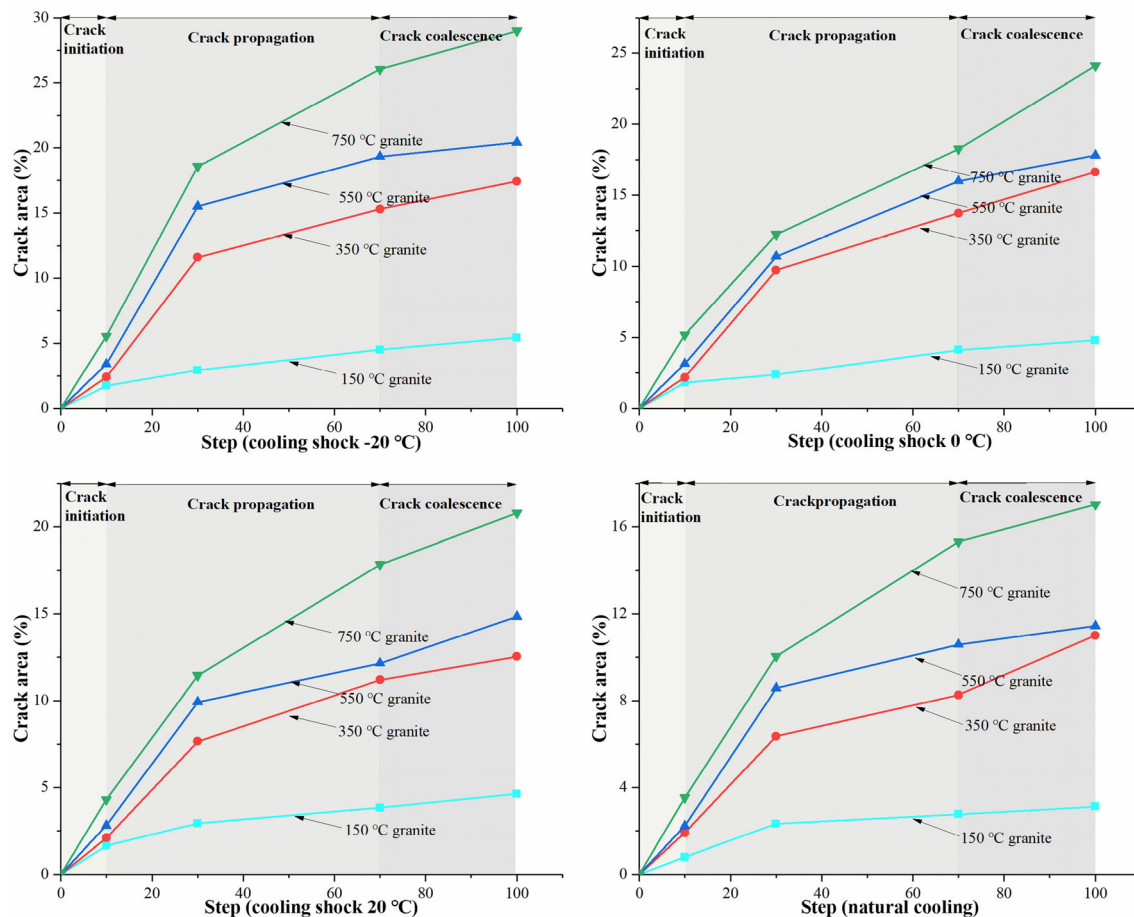

Fig. 4 Real-time ratio of surface cracks in the process of cooling shock crack growth

temperature difference between the rock temperature and the refrigerant temperature led to a larger proportion of cracks on the rock surface and faster crack propagation, indicating that cooling shocks can significantly improve the crack density and propagation rate in high-temperature rocks.

Discussion

Deviation analysis between experiment and numerical simulation

Two laboratory experiments and RFPA^{2D}-Thermal methods were combined to analyze the cooling shock crack propagation process. Both well reflected the thermal cracking phenomenon of high-temperature polymers under cooling shocks: a lower cooling shock temperature and higher granite temperature corresponded to better crack propagation and coalescence (longer and wider cracks) and more severe deterioration of the rock. However, further investigation revealed a difference between the two. For the laboratory experiments, the rock at 150 °C did not exhibit the phenomenon of cracks under the cooling shock, which is consistent with the experimental results of Chen et al. (2017). Microcracks appeared in granite at 350 °C, but this experimental phenomenon was not obvious. The formation of cracks in the 550 and 750 °C granite under cooling shocks was more obvious. Localized open-type cracks were observed. The cracks in the 550 °C granite group generally extended along the mineral particles, producing ring cracks. The cracks of the 750 °C granite group expanded further, becoming long radial cracks. In the RFPA^{2D}-Thermal simulation experiment, the 150 °C granite formed mostly dense short cracks. For the 350 °C granite, microcracks and microholes constantly propagated, contributing to long crack. The main and secondary cracks interconnected, forming a dense network of short through cracks in the 550 °C granite, with small local cavities. However, in the 750 °C granite, the through cracks propagated into a large number of hollow structures, and the rock particles fell off and exhibited fragmental shapes. Additionally, the rock deteriorated significantly.

To further investigate the difference between the experiments and numerical simulations, the surface cracking rate of the high-temperature granite under different cooling shocks was quantitatively analyzed (Fig. 5; the dotted and solid lines indicate the numerical simulation results and experimental measurements, respectively). In the range of 150–350 °C, the rock was in undamaged or slightly damaged stage, and the development rate of the rock surface cracks was equivalent to that in the simulation. The difference is that at the temperature nodes of 150 and 350 °C, the simulated value generally exceeded the experimental value. For example, when the cooling shock temperature was –20 °C, the proportion of
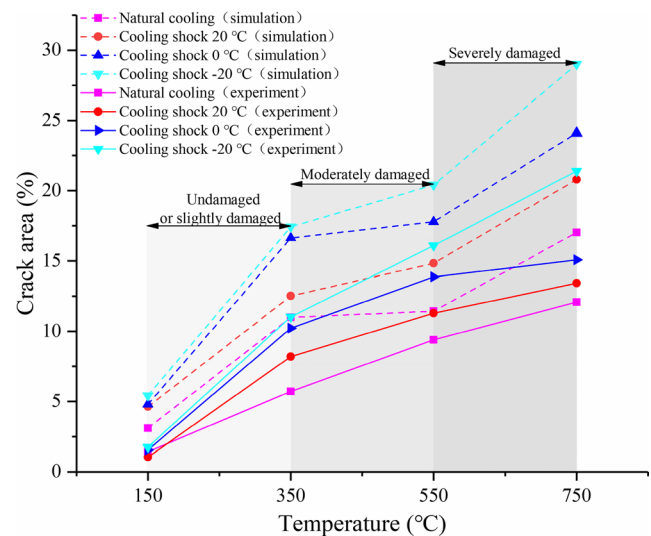

Fig. 5 Comparison of the cracking rate between the laboratory experiment and the RFPA^{2D}-Thermal simulation

granite surface cracks was only 1.77% for the 150 °C granite, whereas the simulated value was 5.43%; for the 350 °C granite, the proportion of surface cracks was only 11.04%, compared with the simulated value of 17.43%. In the range of 350–550 °C, the rock was in a moderately damaged stage. The growth of the simulation value slowed, but the measured value increased rapidly, indicating that the cooling shock cracking effect of rocks was the most significant in this temperature range, and the surface cracking rate of rocks remained relatively high in the simulation. In the range of 550–750 °C, the rock was in a severely damaged stage. Compared with the experimental value, the crack growth rate in the simulation was significantly higher. When a cooling shock of –20 °C was applied to the 750 °C granite, compared with the laboratory experiment, the cracking rate in the simulation increased by 9%; the increase was 9.02% under a cooling shock of 0 °C, 7.37% under a cooling shock of 20 °C, and 4.94% under the natural cooling temperature.

According to the foregoing analysis and discussion, the differences between the laboratory experiment and simulation were mainly attributed to the following two aspects. (1) There were various physical fields interacting in the rock, and the actual rock composition and internal structure were complex. However, the numerical simulation was simplified, with various assumptions, which resulted in the aforementioned differences and generally made the simulation values higher than the measured values. (2) When the cooling shocks acted on the high-temperature granite, cracks were formed inside the rock; however, owing to the experimental instruments and other factors, only the surface cracks of the rock samples were considered. The internal cracks of the rock were not counted, and the percentage of cracks on the rock surface was used to represent the proportion of cracks in the whole rock; to some extent, it can reflect the crack propagation of the rock, but

there is still a deviation, which led to the differences between the results of the experiment and the numerical simulation.

Mechanism analysis of crack propagation in high-temperature rock under cooling shocks

The granitic particles are large, and their crack development mode is consistent with the tip catastrophe model; that is, stress concentration occurs at the tip of the cavity or microcrack, forcing the stress concentration area to expand to the surrounding weaker part, which results in large interconnected cracks. A schematic of the evolution process is shown in Fig. 6 (Sun et al. 2014). Initiation stage: after the rock is heated, its internal rock particles are in the thermal equilibrium state of high-temperature expansion. When the refrigerant is suddenly injected, the rock in contact with the refrigerant (the rock at the cooling shock boundary) instantly undergoes extremely high-temperature changes, and the resulting thermal stress destroys the weakest part of the matrix connecting the mineral particles, resulting in mineral particle cracks and causing particles to peel off. At this time, the sample boundary of the rock is at room temperature (25 °C), which is still a low-temperature environment relative to the heated rock. The temperature difference formed causes crack propagation at the sample boundary. The internal and external cracks are predominantly distributed along the vertical maximum principal stress direction. The initiating cracks are mostly perpendicular to the boundary of the rock sample and start to expand inward; according to the theory of the shortest distance of the plastic zone of the composite mode crack fracture, the energy consumption is the lowest (Kim et al. 2014). Propagation stage: With the internal and external cooling shock temperature field moving to the interior of the rock, the high-temperature granite minerals undergo cold shrinkage,

and the core area remains in a state of high-temperature expansion; that is, under a very high-temperature gradient, tensile shear stresses are developed on the rock surface, and new microcracks are generated inside the sample when the thermal stresses exceed the thermal stress limit of the structure. With the cooling process transferring from the boundary to the interior of the model, the crack further expands under the effect of stress concentration at the crack tip (Tang et al. 2020). Moreover, owing to the different thermal expansion coefficients of various rock-forming mineral particles and the uneven distribution of the particles in the rock, the particles cannot freely expand and contract (they are constrained by each other), and the thermal stress inside the rock forms secondary cracks. With the thermal stress conduction to the inner part of the rock, the primary and secondary cracks combine, and the cracks in the rock gradually expand, forming a larger crack. In the coalescence stage, the temperature field of the cooling shock moves quickly to the interior of the rock, while the room-temperature field at the sample boundary moves slowly to the interior of the rock, resulting in the phenomenon that the length and width of the internal crack are larger than those of the external crack. With the internal and external temperature fields moving to the interior of the rock, the two temperature fields meet near the sample boundary. The thermal equilibrium zone inside the rock is destroyed, and the internal and external cracks combine. A rock model group with a larger temperature gradient exhibits the formation of more local cavity structures.

With an increase in the rock temperature, the crack propagation and rock degradation effect became more obvious. The evolution is shown in Fig. 7. The temperature difference between the rock model at 150 °C and the cooling shock temperature was small, and the thermal stress generated was insufficient to completely connect the internal and external cracks,
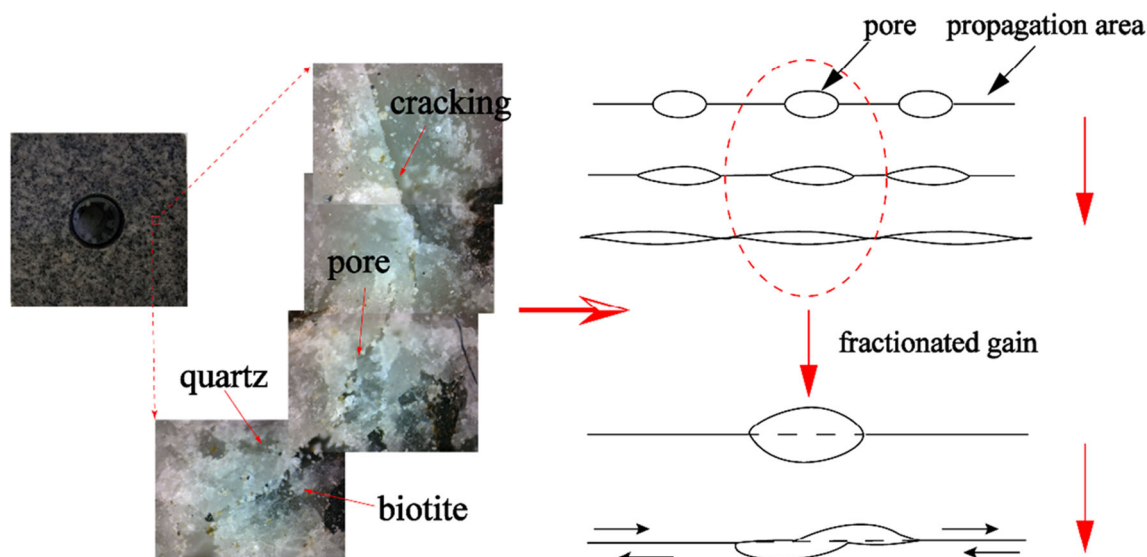

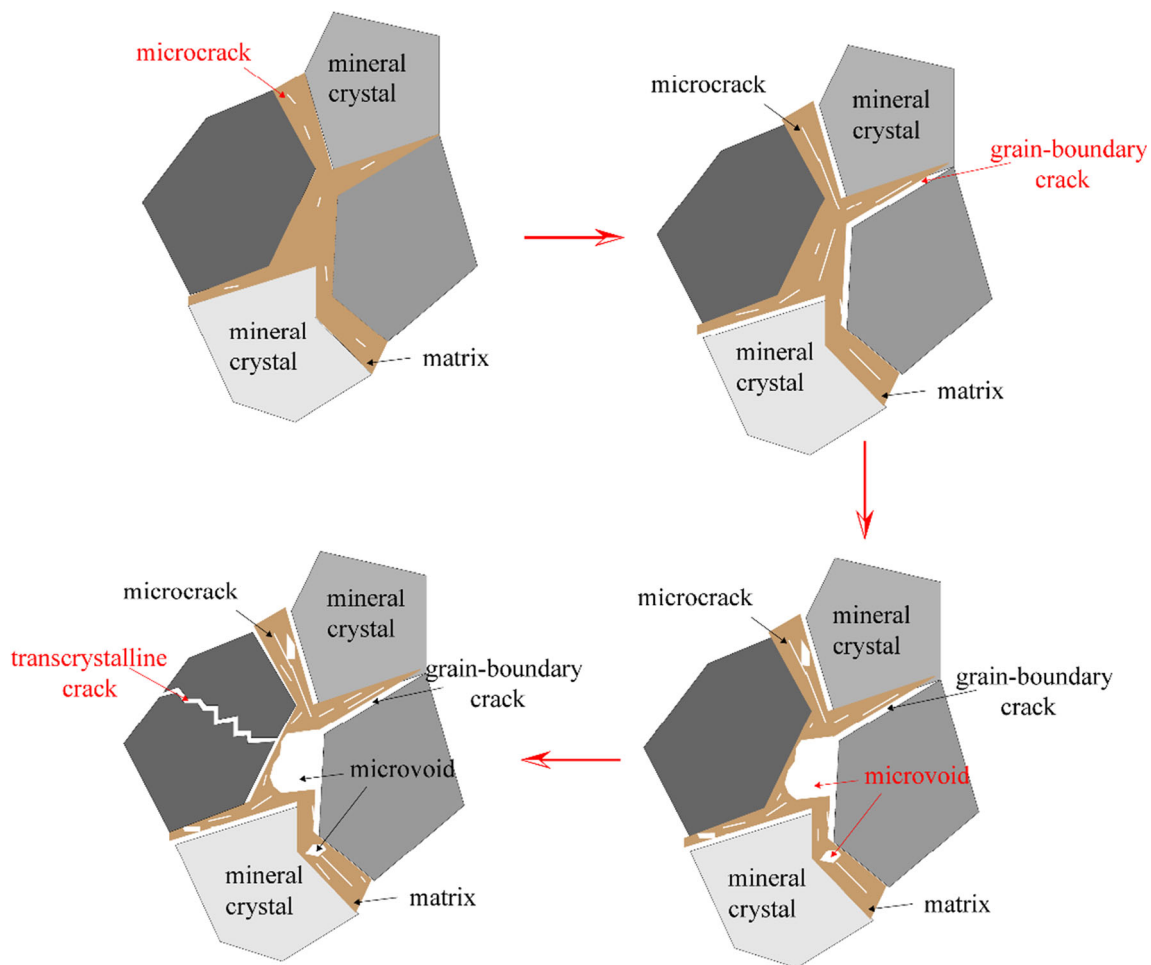**Fig. 6** Rock crack evolution diagram (Sun et al. 2014)

Fig. 7 Evolution of the cooling shock crack growth in high-temperature granite

which led to the inner and outer cracks not fully penetrating at 150 °C. Additionally, there was always a ring-shaped stress-balance zone. Because of the complexity of thermal expansion, the densification stage of the thermally induced microcracks was longer for the 350 °C rock, which increased the crack density rapidly. Under the action of a large temperature gradient, the high thermal stress generated in the rock caused the stress-weak areas within the rock are broken. This is because cracks tend to propagate well along the preferred path, mainly along grain boundaries and large quartz, biotite minerals, and minerals with microcracks spread, forming a small range of damage areas (Kumari et al. 2018b). Furthermore, the distribution and types of minerals in the rocks were different; the uneven expansion of high-temperature rock particles resulted in uncoordinated deformation, which aggravated the crack propagation. Additionally, the organic matter in granite cement and ore-forming minerals (attached water, bound water, and crystal water) caused high-temperature dissociation and melting reaction in this temperature range, and the crack development was along the boundaries of mineral crystal particles, which aggravated the fracture of the rock. The crack propagation in the granite at 550 and 750 °C was relatively rapid under cooling shocks. The cracks

combined, forming transcrystalline cracks. The rock was broken into small blocks and clastics structure over a large area, and there were many voids in the rock and hollow structure. Between 500 and 600 °C, the minerals in granite (wolframite, siderite, magnetite, pyrrhotite, pyrite, illite, kaolinite, etc.) undergo chemical changes, which are characterized by a volume increase, bearing-capacity decrease, connectivity increase, wave-velocity mutation, etc. (Sun et al. 2015) Additionally, granite contains a large amount of quartz (37.9% for Ganzi granite, 25.8% for Westerly granite), and the transition temperature of the α and β phases of quartz is approximately 573 °C (Glover et al. 1995; Smalley and Markovic 2017). During the heat treatment, the quartz changes from the alpha (α) phase to the beta (β) phase. When granite samples with high temperatures of 550 and 750 suffering from different cooling shocks, all these rock ones would cooled rapidly, and the quartz changed from the β phase to the α phase. After two state transformations, a large amount of quartz in the rock formed large local pores and cavities around the mineral particles, which aggravated the deterioration of the rock.

Conclusions

Temperature shock is an important factor affecting the stability of engineering. The fracture law of high-temperature granite under different cooling shocks was studied in laboratory experiments. Additionally, the cooling shock-induced crack propagation was analyzed using RFPA^{2D}-Thermal. The main conclusions are as follows:

(1) The laboratory experiments revealed that for 150–350 °C granite, the rock was undamaged or slightly damaged, the microcracks were mostly propagated inside the granite, and the surface macrocracks were not obvious. For 350–550 °C granite, the rock was moderately damaged, there was a temperature critical value for the sudden change in the crack macroscopic shape, a large number of open cracks appeared on the rock surface, and the amount of thermal damage was significantly increased. The 550–750 °C granite was severely damaged; the rock cracks further expanded, forming radial open-type long cracks.

(2) Under the cooling shocks, the crack initiation in the high-temperature granite started at the boundary of the cooling shock hole and the sample. The cracks extended radially to the interior of the rock, and the distance between the medium length crack and long cracks was almost equal. In the process of crack propagation, there was always a ring-shaped equilibrium zone inside the rock, along with many short cracks on the rock surface.

(3) The weakest part of the matrix between rock particles was destroyed first, and numerous microcracks were produced. Then, the distribution and types of minerals in the rock caused the uneven expansion of high-temperature rock particles. The generated thermal stress promoted the crack propagation. The cracks were mostly formed along the boundary of mineral crystal particles, resulting in a local failure zone.

(4) A larger temperature gradient inside the rock corresponded to a higher crack propagation rate, larger penetration range, and higher density of cooling shock-induced cracks. The results indicate that the drilling efficiency for geothermal resource development and high-temperature rock masses can be improved by increasing the temperature gradient and injection rate of the cooling shock fluid.

Author contribution Y.-j.S. and J.-s.H. conceived and designed the experiments; J.-s.H., J.-q.Y., and X.H performed the experiments; J-s H, X.H, J.-q.Y., and Z-p B analyzed the data; Y.-j.S. contributed funding supports; J.-s.H. wrote the paper; and Y.-j.S. revised the English of this paper.

Declarations

Conflict of interest   The authors declare no competing interests.

References

Akdag S, Karakus M, Taheri A, Nguyen G, Manchao H (2018) Effects of thermal damage on strain burst mechanism for brittle rocks under true-triaxial loading conditions. Rock Mech Rock Eng. 1007/s00603-018-1415-3

Akdag S, Karakus M, Nguyen GD, Taheri A (2020) Strain burst vulnerability criterion based on energy-release rate. Eng Fract Mech 107232. 10.1016/j.engfracmech.2020.107232

Bažant ZP, Ohtsubo H, Aoh K (1979) Stability and post-critical growth of a system of cooling or shrinkage cracks. Int J Fract 15(5):443–456. https://doi.org/10.1007/BF00023331

Cai M, Kaiser PK, Tasaka Y, Maejima T, Morioka H, Minami M (2004) Generalized crack initiation and crack damage stress thresholds of brittle rock masses near underground excavations. Int J Rock Mech Min Sci 41(5):833–847. https://doi.org/10.1016/j.ijrmms.2004.02.001

Cha M, Yin X, Kneafsey T, Johanson B, Alqahtani N, Miskimins J, Patterson T, Wu Y-S (2014) Cryogenic fracturing for reservoir stimulation – laboratory studies. J Pet Sci Eng 124:436–450. https://doi.org/10.1016/j.petrol.2014.09.003

Chen S, Yang C, Wang G (2017) Evolution of thermal damage and permeability of Beishan granite. Appl Therm Eng 110:1533–1542. https://doi.org/10.1016/j.applthermaleng

Cui F, Zhang T, Lai X, Cao J, Shan P (2019) Study on the evolution law of overburden breaking angle under repeated mining and the application of roof pressure relief. Energies 12(23):4513. https://doi.org/10.3390/en12234513

Dalian Mechsoft Co L (2016) Realistic failure process analysis. Journal of Rock Mechanics & Geotechnical Engineering. https://doi.org/CNKI: SUN: JRMG.0.2016-03-016

Diederichs MS, Kaiser PK, Eberhardt E (2004) Damage initiation and propagation in hard rock during tunnelling and the influence of near-face stress rotation. Int J Rock Mech Min Sci 41(5):785–812. https://doi.org/10.1016/j.ijrmms.2004.02.003

Feng G, Wang X, Wang M, Kang Y (2020) Experimental investigation of thermal cycling effect on fracture characteristics of granite in a geothermal-energy reservoir. Eng Fract Mech 235. https://doi.org/10.1016/j.engfracmech.2020.107180

Gao F-Q, Stead D, Elmo D (2016) Numerical simulation of microstructure of brittle rock using a grain-breakable distinct element grain-based model. Comput Geotech 78:203–217. https://doi.org/10.1016/j.compgeo.2016.05.019

Ghamartale A, Escrochi M, Riazi M, Faghih A (2019) Experimental investigation of ultrasonic treatment effectiveness on pore structure. Ultrason Sonochem 51:305–314. https://doi.org/10.1016/j.ultsonch.2018.10.002

Glover PWJ, Baud P, Daro M, Meredith PG, Boon SA, Leravalec M, Zoussi S, Reuschlé T (1995) α/β phase transition in quartz

monitored using acoustic emissions. Geophys J Int 120(3):775–782. https://doi.org/10.1111/j.1365-246X.1995.tb01852.x

Huang ML, Tang CA, Liang ZZ (2001) Stress field analysis of interaction of rock cracks. Journal of Northeastern University 04:446–449. https://doi.org/10.3321/j.issn:1005-3026.2001.04.025

Huang Z-W, Wu X-G, Li R, Zhang S-K, Yang R-Y (2019) Mechanism of drilling rate improvement using high-pressure liquid nitrogen jet. Pet Explor Dev 046(004):768–775. https://doi.org/10.1016/S1876-3804(19)60239-9

Huang Y-H, Yang S-Q, Bu Y-S (2020) Effect of thermal shock on the strength and fracture behavior of pre-flawed granite specimens under uniaxial compression. Theor Appl Fract Mech 106:102474. https://doi.org/10.1016/j.tafmec.2020.102474

Isaka B, Gamage R, Rathnaweera T, Perera M, Chandrasekharam D, Kumari W (2018) An influence of thermally-induced micro-cracking under cooling treatments. Mechanical Characteristics of Australian Granite 11(6):1338. https://doi.org/10.3390/en11061338

Kim K, Kemeny J, Nickerson M (2014) Effect of rapid thermal cooling on mechanical rock properties. Rock Mech Rock Eng 47:2005–2019. https://doi.org/10.1007/s00603-013-0523-3

Kumari W, Ranjith P, Perera M, Chen B (2018a) Experimental investigation of quenching effect on mechanical, microstructural and flow characteristics of reservoir rocks: thermal stimulation method for geothermal energy extraction. J Pet Sci Eng 162:419–433. https://doi.org/10.1016/j.petrol.2017.12.033

Kumari W, Ranjith P, Perera M, Li X, Li L, Chen B, Isaka B, De S (2018b) Hydraulic fracturing under high temperature and pressure conditions with micro CT applications. Geothermal Energy from Hot Dry Rocks 230(15):138–154. https://doi.org/10.1016/j.fuel.2018.05.040

Li J-C, Zhao W-C, Liu S-Q (2019) Description of shale pore fracture structure based on multi-fractal theory. Advances in Petroleum Exploration and Development 18(1):1–9. https://doi.org/10.3968/11342

Lin, W (2002) Permanent strain of thermal expansion and thermally induced microcracking in Inada granite. J Geophys Res 107. https://doi.org/10.1029/2001JB000648

Liu C, Shi B, Zhou J, Tang C (2011) Quantification and characterization of microporosity by image processing, geometric measurement and statistical methods: application on SEM images of clay materials. Applied Clay ence 54:97–106. https://doi.org/10.1016/j.clay.2011.07.022

Liu C, Tang C, Tang S, Suo W (2013) Automatic quantification of crack patterns by image processing. Comput Geosci 57:77–80. https://doi.org/10.1016/j.cageo.2013.04.008

Liu T, Lin B, Zou Q, Zhu C, Guo C, Li J (2015) Investigation on mechanical properties and damage evolution of coal after hydraulic slotting. J Nat Gas Sci Eng 24:489–499. https://doi.org/10.1016/j.jngse.2015.04.016

Liu J-R, Li B-Y, Tian W, Wu X-G (2018) Investigating and predicting permeability variation in thermally cracked dry rocks. Int J Rock Mech Min Sci 103:77–88. https://doi.org/10.1016/j.ijrmms.2018.01.023

Liu L, Xin J, Huan C, Qi C C, Zhou W W, Song KI-IL (2020) Pore, and strength characteristics of cemented paste backfill using sulphide tailings: effect of sulphur content. Constr Build Mater 237. 10.1016/j.conbuildmat.2019.117452

Lyu Z, Song X, Li G, Wang G, Shi Y, Liu Y, Zheng R (2018) Experimental analysis on characteristics of micro-structure and mineralogy changes in thermal spallation drilling. J Pet Sci Eng 167:100–109. https://doi.org/10.1016/j.petrol.2018.03.107

Miao S, Pan PZ, Zhao X et al (2020) Experimental study on damage and fracture characteristics of Beishan granite subjected to high-temperature treatment with DIC and AE techniques. Rock Mech Rock Eng 1–3:1–23. https://doi.org/10.1007/s00603-020-02271-4

Piane CD, Arena A, Sarout J, Esteban L, Cazes E (2015) Micro-crack enhanced permeability in tight rocks: an experimental and microstructural study. Tectonophysics: International Journal of Geotectonics and the Geology and Physics of the Interior of the Earth 665:149–156. https://doi.org/10.1016/j.tecto.2015.10.001

Qin L, Zhai C, Liu SM, Xu SJ, Dong RW (2018) Fractal dimensions of low rank coal subjected to liquid nitrogen freeze-thaw based on nuclear magnetic resonance applied for coalbed methane recovery. Powder Technol 325:11–20. https://doi.org/10.1016/j.powtec.2017.11.027

Shen Y-J, Hou X, Yuan J-Q, Zhao C (2019) Experimental study on temperature change and crack expansion of high temperature granite under different cooling shock treatments. Energies 12(11). https://doi.org/10.3390/en12112097

Shen Y-J, Hou X, Yuan J-Q, Wang S-F, Zhao C-H (2020a) Thermal cracking characteristics of high-temperature granite suffering from different cooling shocks. Int J Fract. https://doi.org/10.1007/s10704-020-00470-2

Shen Y-J, Hou X, Yuan J-Q, Xu Z, Hao J-S, Gu L, Liu Z (2020b) Thermal deterioration of high-temperature granite after cooling shock: multiple-identification and damage mechanism. Bull Eng Geol Environ. https://doi.org/10.1007/s10064-020-01888-7

Shi X-C, Gao L, Wu J, Zhu C, Chen S, Zhuo X (2020) Effects of cyclic heating and water cooling on the physical characteristics of granite. Energies 13(9). https://doi.org/10.3390/en13092136

Siratovich P, Villeneuve C, Marlène C, Cole J, Kennedy B, Bégué F (2015) Saturated heating and quenching of three crustal rocks and implications for thermal stimulation of permeability in geothermal reservoirs. International Journal of Rock Mechanics & Mining ences 80:265–280. https://doi.org/10.1016/j.ijrmms.2015.09.023

Smalley I, Markovic S (2017) Controls on the nature of loess particles and the formation of loess deposits. Quat Int 502:160–164. https://doi.org/10.1016/j.quaint.2017.08.021

Sun Q, Qin F, Xue L, Yu P, Li H, Zhu S (2014) Critical phenomenon and information identification of rock destruction. China Mining University Press 11.

Sun Q, Zhang W, Xue L, Zhang Z, Su T (2015) Thermal damage pattern and thresholds of granite. Environ Earth Sci 74(3):2341–2349. https://doi.org/10.1007/s12665-015-4234-9

Tang C-A, Lin-P WR, Chau K-T (2001) Analysis of crack coalescence in rock-like materials containing three flaws - Part II: numerical approach. Int J Rock Mech Min Sci 38. https://doi.org/10.1016/S1365-1609(01)00065-X

Tang SB, Tang CA, Zhu WC, Wang SH, Yu QL (2006) Numerical investigation on rock failure process induced by thermal stress. Chin J Rock Mech Eng 25(10):2017–2078. https://doi.org/10.3321/j.issn:1000-6915.2006.10.019

Tang CA, Tang SB, Gong B, Bai HM (2015) Discontinuous deformation and displacement analysis: from continuous to discontinuous. Sci China Technol Sci 58(09):1567–1574. https://doi.org/10.1007/s11431-015-5899-8

Tang SB, Zhang H, Tang CA, Liu H (2016) Numerical model for the cracking behavior of heterogeneous brittle solids subjected to thermal shock. Int J Solids Struct 80:520–531. https://doi.org/10.1016/j.ijsolstr.2015.10.012

Tang S-B, Wang J-X, Chen P-Z (2020) Theoretical and numerical studies of cryogenic fracturing induced by thermal shock for reservoir stimulation. Int J Rock Mech Min Sci 125:104160. https://doi.org/10.1016/j.ijrmms.2019.104160

Wang F, Konietzky H (2019) Thermo-mechanical properties of granite at elevated temperatures and numerical simulation of thermal cracking. Rock Mech Rock Eng 52(10):3737–3755. https://doi.org/10.1007/s00603-019-01837-1

Weng L, Wu Z, Liu Q (2020) Influence of heating/cooling cycles on the micro/macrocracking characteristics of Rucheng granite under

unconfined compression. Bull Eng Geol Environ 79:1289–1309. https://doi.org/10.1007/s10064-019-01638-4

Wu Q, Weng L, Zhao Y, Guo B, Luo T (2019) On the tensile mechanical characteristics of fine-grained granite after heating/cooling treatments with different cooling rates. Eng Geol 253:94–110. https://doi.org/10.1016/j.enggeo.2019.03.014

Xu X, Gao F, Zhang Z (2014) Influence of confining pressure on deformation and strength properties of granite after high temperatures. Chinese J Geot Eng 36(12):2246–2252. https://doi.org/10.11779/CJGE201412012

Zhang X-P, Liu Q-S, Wu S-C, Tang X-H (2015) Crack coalescence between two non-parallel flaws in rock-like material under uniaxial compression. Eng Geol 199:74–90. https://doi.org/10.1016/j.enggeo.2015.10.007

Zhang Z-B, Li X, He J-M, Wu Y-S, Li G-F (2017) Numerical study on the propagation of tensile and shear fracture network in naturally fractured shale reservoirs. J Nat Gas Sci Eng 37:1–14. https://doi.org/10.1016/j.jngse.2016.11.031

Zhang L, Li B, Zhang Q, Ren Y (2018a) Study on pore damage and permeability evolution properties of coal rock caused by liquid nitrogen soaking. Chin J Rock Mech Eng 37:3938–3946. https://doi.org/10.1002/ese3.505

Zhang Y, Wong L, Ngai Y (2018b) A review of numerical techniques approaching microstructures of crystalline rocks. Comput Geosci. https://doi.org/10.1016/j.cageo.2018.03.012

Zhao Z, Zhou X-P (2020) 3D digital analysis of cracking behaviors of rocks through 3D reconstruction model under triaxial compression. J Eng Mech 146(8):04020084. https://doi.org/10.1061/(ASCE)EM.1943-7889.0001822

Zhao Z, Liu Z, Pu H, Li X (2018) Effect of thermal treatment on Brazilian tensile strength of granites with different grain size distributions. Rock Mech Rock Eng 51:1293–1303. https://doi.org/10.1007/s00603-015-0712-3

Zhou X-P, Li G-Q, Ma H-C (2020) Real-time experiment investigations on the coupled thermomechanical and cracking behaviors in granite containing three pre-existing fissures. Eng Fract Mech 224. https://doi.org/10.1016/j.engfracmech.2019.106797

Zhu WC, Tang CA, Yang TH, Liang ZZ (2003) Constitutive relationship of mesoscopic elements used in RFPA^{2D} Its Validation. Chin J Rock Mech Eng 2003(01):24–29. https://doi.org/10.3321/j.issn:1000-6915.2003.01.004

Zhu D, Jing H, Yin Q, Han G (2018) Experimental study on the damage of granite by acoustic emission after cyclic heating and cooling with circulating water. Processes 6(8). https://doi.org/10.3390/pr6080101

Zhu X-Z, Hu Y-Q, Jin, P-H, Zhao G-K, Li C (2019) Effect of granite thermal conductivity on the heat-flow coupling heat exchange efficiency of fractures. Mining Research and Development 39(10):47-51. 10.13827/j.cnki.kyyk.2019.10.010